Applied Energy 204 (2017) 994–1006

Contents lists available at ScienceDirect

Applied Energy

journal homepage: www.elsevier.com/locate/apenergy

Novel hybrid CSP-biomass CHP for flexible generation: Thermo-economic analysis and profitability assessment

Antonio M. Pantaleo [a,d,e,*], Sergio M. Camporeale [b], Adio Miliozzi [c], Valeria Russo [c], Nilay Shah [d], Christos N. Markides [d,e]

[a] Department of Agro-Environmental Sciences, Università degli Studi di Bari, Via Amendola 165/A, 70125 Bari, Italy
[b] Dipartimento DMMM, Politecnico di Bari, Via Orabona 4, 70125 Bari, Italy
[c] Energy Technologies Department, ENEA, Casaccia Research Centre, Via Anguillarese, 301. 00123 S.M. di Galeria, Rome, Italy
[d] Centre for Process Systems Engineering (CPSE), Imperial College London, South Kensington Campus, London SW7 2AZ, UK
[e] Clean Energy Processes (CEP) Laboratory, Imperial College London, South Kensington Campus, London SW7 2AZ, UK

HIGHLIGHTS

- A novel hybrid CSP/biomass combined cycle is modelled in Cycle-tempo.
- Input data for costs and profitability assessment are taken from real pilot plants.
- Thermal storage, collectors sizing and operational strategies are compared.
- CSP integration increases efficiency but not investment profitability.

ARTICLE INFO

Article history:
Received 13 January 2017
Received in revised form 11 April 2017
Accepted 3 May 2017
Available online 12 May 2017

Keywords:
Thermo-economic analysis
EFGT
ORC
Biomass
Cycle-tempo
Concentrating solar power

ABSTRACT

This paper focuses on the thermo-economic analysis of a 2.1-MWe and 960 kWt hybrid solar-biomass combined heat and power (CHP) system composed of a 1.4-MWe Externally Fired Gas-Turbine (EFGT) and a 0.7-MWe bottoming Organic Rankine Cycle (ORC) power plant. The primary thermal energy input is provided by a hybrid Concentrating Solar Power (CSP) collector array covering a total ground area of 22,000–32,000 m^2, coupled to a biomass boiler. The CSP collector array is based on parabolic-trough concentrators (PTCs) with molten salts as the heat transfer fluid (HTF), upstream of a 4.5–9.1 MWt fluidized-bed furnace for direct biomass combustion. In addition, two molten-salt tanks are considered that provide 4.8–18 MWh (corresponding to 1.3–5.0 h) of Thermal Energy Storage (TES), as a means of reducing the variations in the plant's operating conditions, increasing the plant's capacity factor and total operating hours (from 5500–6000 to 8000 h per year). On the basis of the results of the thermodynamic simulations, upfront and operational costs assessments, and considering an Italian energy policy scenario (feed-in tariffs, or FiTs, for renewable electricity), the global energy conversion efficiency and investment profitability of this plant are estimated for different sizes of CSP and biomass furnaces, different operation strategies (baseload and modulating) and cogenerative *vs.* electricity-only system configurations. Upfront costs in the range 4.3–9.5 MEur are reported, with operating costs in the range 1.5–2.3 MEur annually. Levelized costs of energy from around 100 Eur/MWh to above 220 Eur/MWh are found, along with net present values (NPVs) from close to 13,000 to −3000 kEur and internal rates of return (IRRs) from 30% down to almost zero when prioritizing electrical power generation (i.e., not in cogenerative mode). In all cases the economic viability of the systems deteriorate for larger CSP section sizes. The results indicate the low economic profitability of CSP integration in comparison to biomass-only plants, due to high investment costs of the former, which are not compensated by the higher global energy conversion efficiency and energy sales revenues.
© 2017 The Authors. Published by Elsevier Ltd. This is an open access article under the CC BY license (http://creativecommons.org/licenses/by/4.0/).

1. Introduction

Decentralized, renewable, cogenerative power plants can contribute towards the EU energy policy targets of sustainable, secure

* Corresponding author at: Department of Agro-Environmental Sciences, Università degli Studi di Bari, Via Amendola 165/A, 70125 Bari, Italy.
E-mail addresses: antonio.pantaleo@uniba.it, a.pantaleo@imperial.ac.uk (A.M. Pantaleo).

http://dx.doi.org/10.1016/j.apenergy.2017.05.019
0306-2619/© 2017 The Authors. Published by Elsevier Ltd.
This is an open access article under the CC BY license (http://creativecommons.org/licenses/by/4.0/).

Acronyms

A	heat exchanger area
ANI	Aperture Normal Irradiance (normal to the aperture plane)
CHP	combined heat and power
CSP	Concentrating Solar Power
DNI	Direct Normal Insolation (direct beam solar radiation on a plane normal to the sun's rays)
EFGT	Externally-Fired Gas Turbine
FiT	Feed-in-Tariff
HTF	heat transfer fluid
HTHE	High-Temperature Heat Exchanger (between the flue gases and compressed air flow into the EFGT)
IAM	Incidence Angle Modifier (optical characteristic affecting performance)
IRR	Internal Rate of Return
LCOE	Levelized Cost of Energy
LM	Logarithmic Mean (of the heat exchanger temperature difference ΔT)
MM	Hexamethyldisiloxane (working fluid of the ORC)
NPV	Net Present Value
ORC	Organic Rankine Cycle
PTC	parabolic-trough collector
TES	thermal energy storage
U	overall heat transfer coefficient

and competitive energy supply [1,2]. In this context, hybrid concentrating solar power (CSP) and biomass-fired combined heat and power (CHP) plants are a promising solution for the efficient and dispatchable generation of heat and power. CSP technologies generate electricity by concentrating the incident solar radiation onto a small area, where a heat transfer fluid (HTF) is heated. This thermal energy is then transferred to a power-generation system. The integration of thermal energy storage (TES) in CSP systems can make CSP dispatchable and increase their energy conversion efficiency and flexibility [3]. Nevertheless, solar energy is inherently intermittent, such that even with TES the capacity factor of solar power plants is low; in response, many hybrid solar/fossil-fuelled plants are currently in operation or under development to mitigate this issue. As an alternative to fossil fuels, biomass can be an interesting renewable energy option for hybridization [4]. Although biomass often exhibits seasonal availability and presents specific logistic and supply constraints [5–9] it is complementary, both seasonally and diurnally, with CSP and this hybridization could contribute to overcome the individual drawbacks of these primary energy resources and allows such plants to achieve either base load or flexible operation [10]. In the case of biomass combustion, high temperature heat is available and the possibility of combined cycles is introduced which goes beyond classical solar organic Rankine cycle (ORC) systems [11–13].

In the present paper, which goes beyond the work proposed by the same authors in Ref. [14], a 2.1-MWe combined cycle with a 1.4-MWe biomass-CSP topping Externally-Fired Gas Turbine (EFGT) and 0.7-MWe bottoming ORC plant is investigated, and the energy performance and economic profitability of various configurations of such a system in both power-only generation and cogeneration mode are estimated taking into account the investment and operational costs, the influence of the heat demand and the revenues from electricity sales. In particular, Feed-in-Tariffs (FiTs) available in the Italian energy framework are assumed, and resulting cost/performance data are elaborated taking into account the experience from the CSP pilot-plant built by ENEA within the Archimede project [15]. In more detail, two different CSP sizes and TES capacities are considered, and different operating strategies are compared including baseload operation (constant output power with a modulating biomass combustor) and variable CHP operation (constant biomass reactor output and variable solar energy input). The case studies examined in the present work are summarized in Table 1.

The aim of this paper is to propose a novel hybrid biomass-CSP combined CHP system and to present a thermo-economic methodology suitable for the thermodynamic, thermal and financial appraisal of such a plant in different energy demand segments. The methodology adopts a combination of a solar energy yield assessment, combined cycle thermodynamic modelling and energy efficiency analysis, a simplified representation of the energy demand, a cost assessment and a discounted cash-flow analysis. The paper aims to evaluate if, and at what extent, the investment costs for the CSP section of such a hybrid plant are justified by the increased operational flexibility of the plant, and the increased overall conversion efficiency and electricity sales revenues, in comparison to a 100% biomass(-only) fired power generating plant, while also investigating the influence of TES on the solar share and system's profitability.

Table 1
Case studies analysed in the present work.

Only biomass	**A**	
Solar/CHP operation	Fixed CHP output	Variable CHP output
Small-size CSP/TES	**B**	**D**
Large-size CSP/TES	**C**	**E**

Description of case studies. Case A: 100% biomass input with baseload operation; Cases B and C: fixed power output with modulating biomass boiler to compensate variable solar input; Cases D and E: variable output with fixed biomass input (50% of nominal CHP output).

The originality of the paper lies on the adoption of a novel combined cycle, featuring a parabolic-trough collector (PTC) array and dual-tank TES coupled to a biomass-fired EFGT, which promises the possibility of achieving high energy-conversion efficiencies and solar shares in comparison to benchmark hybrid CSP systems. Conventional CSP hybrid schemes proposed in literature are generally based on steam cycles and the biomass is used in a back-up boiler instead of in a conventional gas-turbine [16,17]. In the present study, a combined cycle based on an EFGT [18] and a bottoming ORC unit allows for higher thermodynamic conversion efficiency relative to conventional steam cycles. Furthermore, the rated power output of the distributed plant considered here is one order lower than typical steam plants (~2 MWe *vs.* ~10 MWe, or higher), which can greatly reduce the biomass supply chain and storage issues [19]. The proposed scheme is also innovative with respect to high-temperature CSP plants that usually make use of a solar tower and gas-steam combined cycle [20]. In that case, the solar power input is integrated with the gas-turbine combustor utilizing natural gas, whereas fully renewable energy sources are adopted here.

Another innovative aspect arises from the adoption of PTCs at relatively high-temperature levels. The PTC is the most commercially proven and low risk solar-collector technology and has better optical efficiency in comparison with tower and Fresnel technology [21,22]. In this work, we propose the use of PTCs with a binary molten-salt mixture (sodium and potassium nitrates) as the HTF

and thermal storage medium. The main feature of this technology is that the maximum temperature in the receiver can be at or even in excess of 500 °C (up to 550 °C). Molten-salt technology allows one to increase the solar input by up to 50% compared to employing thermal oils as HTFs, which limits the maximum temperatures to around 400 °C.

Key advantages of such solar-biomass hybridization for real applications are: (i) lower space requirements for the solar collectors and reduced biomass supply constraints due to lower fuel input requirements, for a fixed plant size; (ii) possibility of adopting an EFGT-ORC combined cycle using solar PTCs instead of more expensive solar towers or dishes; (iii) flexible operation of the system when modulating the biomass contribution and possibility to obtain dispatchable renewable energy from smart integration of intermittent solar and programmable biomass sources; (iv) higher conversion efficiency compared to CSP-only systems at the same plant size/scale (i.e., better use of the solar energy input); and (v) possibility of modulating the heat/power output ratio to match on-site energy demand if smart operation of the bottoming ORC unit is adopted (switch on/off or variable condensing temperature of the bottoming cycle).

On the other hand, some major bottlenecks in the implementation of such a system are: (i) relatively high temperatures in the PTC (up to 500–550 °C), which influences costs and energy efficiency; (ii) reduced efficiency of the biomass furnace and of the hot air heat exchanger when modulating the energy output to match the solar input (due to part load operation); and (iii) high solidification temperatures of the molten salts adopted as the HTF and TES media, which requires suitable heating systems to prevent freezing.

2. Literature review on hybrid CSP-biomass CHP

The hybridization of CSP systems has been widely addressed in literature [23]. Hybridization of solar energy with combined cycles offers specific advantages during the yearly operation. In fact, the most demanding conditions for CCGT technology correlate well to the optimal ambient conditions for CSP, which facilitates the integrated behaviour and efficiency of the ISCC [16,24,25]. Previous works [4,26] showed the convenience of ISCC (Integrated Solar Combined Cycle) using PTC and direct steam generation (DSG) in locations with hard climatology, but economic feasibility is questionable in other climates [24]. In Ref. [27], several ISCC configurations were studied in order to find the best point for adding the solar contribution in the heat recovery steam generator (HRSG), finding that the best choice is to evaporate water with DSG at the high pressure level without preheating or superheating. Similar conclusions are found in Ref. [26] where the authors propose a configuration with DSG in all the pressure levels even removing the evaporators of the HRSG. The same authors also proposed the inclusion of a solar multiple in the solar field in order to increase the yearly solar contribution [28].

CSP hybridization can be performed by retrofitting an existing plant or designing an original one [4,29,30]. Usually, there is more flexibility in designing and optimizing a new system, addressing the design challenges properly. It is thus required to simulate the hybrid system, taking into account technological, thermodynamic and economic issues [31–33]. For design purposes, particular stationary conditions for solar irradiance and ambient temperature are usually adopted, even if these design points could be too optimistic and do not properly reflect the fluctuating behaviour due to daily and seasonal changes of solar irradiance. Some researches on such hybridization systems make use of commercial simulation tools or in-house developed software, which allows a detailed description of all plant components and specific calculations on the solar subsystem [34–36]. With respect to the latter, exhaustive computations for the solar efficiency including mirror area, spillage, blocking and shadowing effects, mirror-tracking strategies have been proposed in literature [24,36,37]. These simulations rely on the detailed model of each plant component, however the large number of parameters to be simultaneously optimized makes it difficult to extract direct information about the main losses in the plant and to plan global strategies for the optimization of the plant design and operation.

A wide literature is available on hybridization configurations and strategies of CSP plants with fossil fuels (in particular natural gas), while a limited attention has been paid on biomass-CSP hybridization. In particular, none of the previous researches in this area have addressed the integration of CSP, based on PTC and molten salt TES, with biomass combustion in EFGT, as proposed in this paper.

In recent years, a number of hybrid CSP-biomass plants have been developed [38–40], where CSP plants are connected to steam turbines, using diathermic oil as HTFs, and are hybridized with biomass boiler units that supply the required thermal energy to the power block enabling electrical production during periods of low solar input. In these applications, hybridization allows a continuous operation of the steam turbine (avoiding daily start-ups and shut-downs), thus facilitating a more efficient and profitable use of the CSP plant section.

Srinivas & Reddy [16] simulated a solar-biomass hybrid regenerative steam Rankine cycle without TES, while Vidal & Martin [25] proposed the integration of biomass gasification to a CSP facility; in this case, the options of using syngas for hydrogen production, for providing thermal energy in a furnace or for power generation in an open Brayton-cycle were compared, with the biomass section coupled to a tower-based CSP plant with a molten salt as the HTF. A general multi-criterion approach for selecting the most suitable CSP technology for hybridization with Rankine cycle power plants using conventional (gas, coal) and alternative (biomass, wastes) fuels was suggested by Peterseim et al. [4], which included key factors such as technology maturity, environmental impact, economics and site-specific solar yield. In Ref. [26], the same authors proposed a methodology for categorizing the level of CSP hybridization depending on the interconnections of the plant components, as applied to biomass, fossil fuel and geothermal hybrid systems. Other solar-biomass hybrid configurations considered in the literature are based on PTCs, backup boilers and Rankine cycles [27,41,42], on the substitution of steam bleed regeneration with water preheating by solar energy [43]. Fresnel collectors were also proposed as solar technology for power generation in hybrid renewable plants [28]. Despite of the lower efficiency with respect to solar tower or linear parabolic collectors, Fresnel collectors represent a more economical alternative, suitable for easier integration in industrial or rural area (for example, on the roof of existing buildings). Supercritical CO_2 cycles were also proposed as thermodynamic cycle for power generation from solar and biomass energy sources. In Ref. [44], design and off-design thermodynamic performance of the system were studied, considering variable solar radiation levels and reporting a peak electric efficiency of 40%. In this research, the integration of biomass made the generation efficiency independent from solar radiation fluctuations, facilitating an efficient and stable utilization of solar energy and biomass. However, the biomass combustion efficiency was not fully addressed and the high temperature of the cycle required air pre-heating with correspondent reduction of conversion efficiency. Moreover, no TES was considered, hence the solar energy share was below 10%, as expected in such cases.

Several other hybridization strategies have been proposed in the literature, such as a central solar tower collector coupled to a 4.5-MWe closed Brayton cycle where the solar fluctuation is com-

pensated by a gas-fired combustion system in order to achieve a stable operation independent of the solar radiation conditions [45] and without thermal storage. The overall thermodynamic cycle efficiency, solar conversion efficiency, solar share and power output have been estimated on the basis of real data for irradiance and external temperature, resulting in a relatively low solar share (around 11%) in summer, mainly due to the lack of storage.

In Ref. [36], a hybrid mini-CSP and biomass system was presented and modelled. The solar field adopted PTCs, while a biogas boiler was used in backup mode and a small-scale ORC power unit converted heat to electricity. The results reported an improved (from 3.4 to 9.6%) annualized global electric efficiency with hybridization. On the other hand, the hybridization promoted energy excess, mostly in the summer months, demonstrating that hybridization significantly reduces, but does not eradicate, the need for TES. In Ref. [46], the integration of a PTC-based CSP to a CHP steam turbine plant fed by sugarcane bagasse was proposed. Solar integration was considered for displacing the high-pressure steam extraction of a condensing-extraction steam turbine via preheating feedwater, and operation in a fuel-economy mode was employed in order to save bagasse during the harvesting period with use of the economized bagasse during the off-season. In this study, the hybridization of CSP with biomass allowed base-load power supply, while solar thermal load facilitated the rational use of seasonal bagasse, improving the export of electricity to the grid. In Ref. [47], a first attempt at an exergo-economic analysis was proposed to assess the levelized costs of energy from thermochemical hybridized gas-CSP plants, hybrid thermochemical fuel conversion plants and for comparing them with corresponding conventional single heat-source systems. In another study of interest, a CSP heat source was adopted in Ref. [48] to drive a biomass gasification process and to feed an IGCC plant. In particular, a two-stage solar-biomass gasification concept was used, with a first stage involving biomass pyrolysis, preheating and steam generation, driven by mid-temperature solar thermal energy via Linear Fresnel Collectors (LFC) which can achieve higher efficiencies than PTCs that operate at higher temperatures. Heliostats were adopted in a second biomass gasification stage, and the gasified syngas as utilized by an advanced gas turbine. By using concentrated solar energy to drive the biomass gasification, solar energy was converted to a fuel in the form of gasified syngas. The two-stage process demonstrated an energy level upgrading ratio of 32.4% compared to 21.6% in one-stage gasification mode, with respect to no solar energy input.

With regard to solar collectors, PTC technology is currently the most commercially proven and reliable option [49,50], allowing medium-to-high temperatures with good thermal efficiency. Nowadays, PTC is implemented using collectors like Eurotrough and Solargenix, and it is a well-proven technology [51,52]. LFCs are a more recent development compared to PTCs, but seem to have some potential to reduce the Levelized Cost of Energy (LCOE) of associated systems [50]. LFC technology is simpler, less expensive and more compact than PTCs but also exhibits a lower optical efficiency. A comparison of PTCs and LFCs in the context of hybrid solar-natural gas application is provided in Ref. [53], where the solar contribution was only used for evaporating water in a CCGT (combined cycle gas turbine), increasing the production of the high-pressure level of the steam generator. The economic analysis reported specific costs of 200 Eur/m^2 and 80–160 Eur/m^2 respectively, for PTCs and LFCs. The results also showed that the proposed evaporative configurations could increase annual performance, with the thermal contribution of PTCs shown to be higher, despite LFRs improving the economic feasibility of the plant due to their lower costs. Tower Collectors (TCs) [50] can reach very high temperatures (high solar concentration) and potentially have better performance than PTCs, but they have more complex management (sun tracking algorithms) in the heliostat field [50] and limited optical performance. All of these technologies could be coupled to molten salts as HTFs to achieve the required temperatures but, at present, PTC technology appears as the most reliable one [54], and is selected herein.

In the case of hybrid CSP-biomass plants with steam-turbine inlet temperatures >500 °C and pressures >100 bar, solar towers emerge as the most suitable option, with direct-steam systems preferred in plants without TES and molten salts preferred in plants with TES. However, no attention has been paid to hybrid CSP plants integrated with gas turbines, and featuring PTCs with source temperatures >430 °C. Most of the applications of this arrangement consider the use of solar towers or dishes as solar collectors, and compressed air as the HTF with internally fired cycle configurations [29,46,55].

Liquid storage media with molten salts or synthetic oils are the most common option for high-temperature TES in CSP, and the two-tank storage system is the most commercially mature technology. Several parabolic trough plants are under development or in operation in Spain and the US use the indirect two-tank thermal energy storage concept. These plants use organic oil as the heat transfer fluid and molten salt as the storage fluid. The adoption of a two-tank molten-salt TES presents lower costs per kWh of storage capacity and reduced space requirements in comparison to diathermic oil; in fact, due to the higher temperature difference available for molten salts with respect to oil, the energy stored per unit volume is higher. A two-tank direct storage (a system in which storage material also acts as HTF) was used in early parabolic trough power plants (Solar Electric Generating System I) [56] and at the Solar Two power tower in California [57]. The same concept has been recently re-considered by ENEA in an effort to develop a new type of PTC power plant, whose demonstration was realized in the Archimedes/ENEL CSP plant in Priolo Gargallo (Italy) [58,59] and also forms part of the system proposed in the present work.

3. Technology description and thermodynamic performance analysis

3.1. Plant layout and thermodynamic analysis

The proposed plant is a combined cycle composed of a topping hybrid CSP-biomass EFGT and a bottoming ORC unit. A schematic of the hybrid CSP-biomass EFGT configuration is shown in Fig. 1, which indicates the main thermodynamic plant-design parameters associated with the rated power output.

The heat input to the plant comes both from solar and biomass energy. The solar section is based on PTCs with molten salts as HTF. A TES system with two tanks (one cold and one hot) of molten salts is adopted in order to reduce the fluctuation of the operating conditions and increase the share of solar input. The topping cycle, an EFGT, already proposed in Ref. [14] for the case with only biomass as energy input, has been chosen for the present work since it is well suited to accommodate for the solar energy input. Air taken from the ambient is compressed in the inter-refrigerated compressor to about 12 bar and exits the compressor at 180 °C. The compressed air is heated firstly by molten salts flowing from the hot to the cold storage of the CSP plant up to 500 °C. Then, air is heated to 800 °C by hot gas produced in the furnace and is transferred to the air flowing in the gas turbine in the High-Temperature Heat Exchanger (HTHE). For a more flexible regulation of the combustion process, combustion air to the furnace is taken from the ambient. In this way, the combustion air flowing to the biomass furnace can be regulated independently from the air flowing in the turbine, in relation to the fluctuations of the solar inputs or variation in the biomass properties (mainly, moisture content, calorific value).

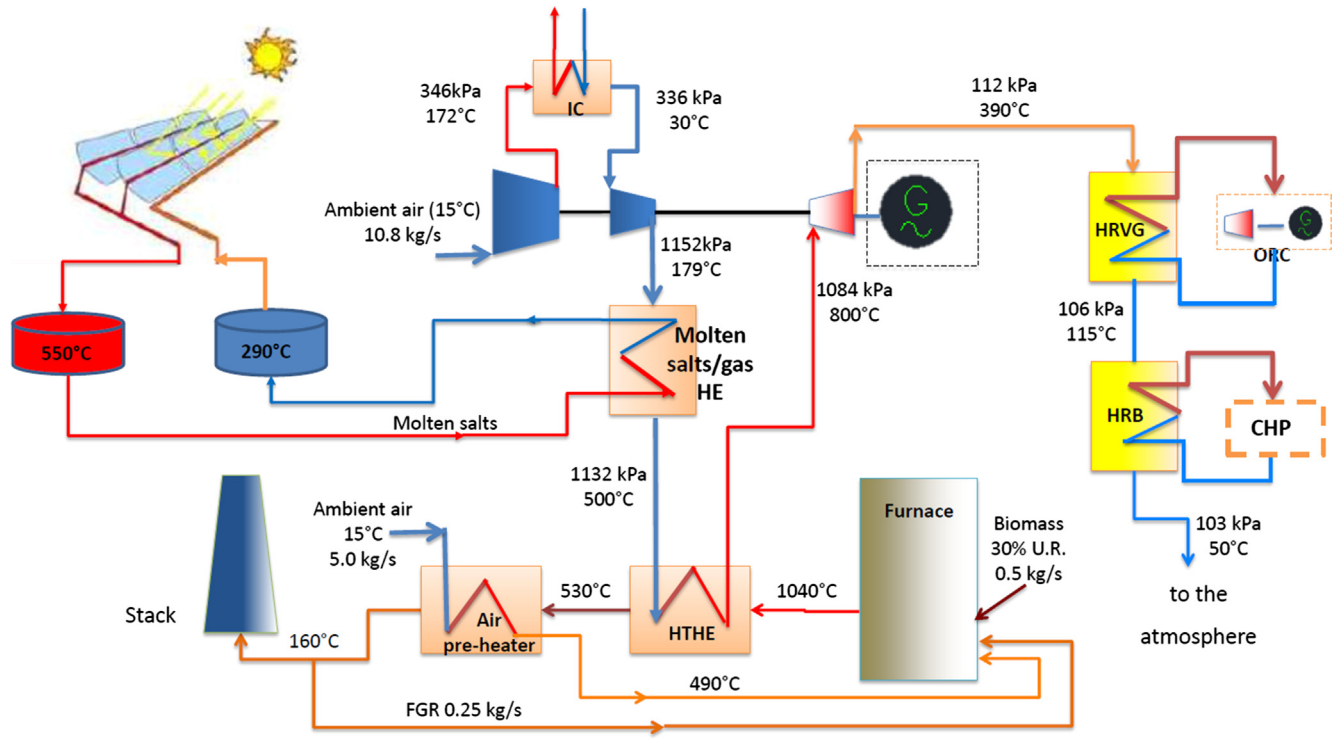

Fig. 1. Layout of the hybrid solar-biomass EFGT-ORC combined cycle power plant. Flow rate, temperature and pressure are referred to rated operating conditions.

However, since the temperature of the compressed air entering the furnace is high (500 °C), pre-heating of the combustion air is needed in order to recover the heat of the exhaust gas. The compressed air exiting the HTHE is expanded in the turbine. At the design point, the turbine exit temperature obtained from calculations is equal to 394 °C.

As shown in Fig. 1, under rated thermal input from the solar plant, the combustion air is pre-heated to 490 °C. Due to the intense air pre-heating, the air-to-fuel ratio need to be relatively high is order to avoid excessive temperature of the combustion gas that may cause biomass ash melting point problems and possible corrosion of the metallic surface of the HTHE. For this reason, the temperature of the combustion gas has been limited to 1040 °C, making also use of a low flue gas recirculation. In such a way, considering that the maximum temperature of the compressed air is limited to 800 °C, the metal temperature remains at a value that allows for the use of nickel–cadmium based heat exchanger. The high air to fuel ratio (air factor $\lambda > 2$) guarantees more efficient combustion with respect to the case without solar input. On the other hand, the thermal losses caused by the sensible heat of the combustion products exhausted to the atmosphere are lowered during hours with solar inputs, due to the lower flow rate of the combustion air.

The heat of the gas exiting the gas turbine is recovered in a Heat Recovery Vapor Generator (HRVG) and transferred to the ORC unit. The air exiting the HRVG is still at a temperature that is suitable for cogeneration. Hence, its sensible heat is recovered in a Heat Recovery Boiler (HRB) for industrial or residential use. In this work, the air is discharged to the atmosphere at 80 °C, assuming that the gas exiting the turbine is pure air without any impurities coming from the combustion process.

The bottoming cycle is an ORC unit in a recuperative configuration (see Fig. 2). In particular, this sub-system contains a pump (6-1) that supplies the fluid to the recuperator (1–2). The recuperator pre-heats the working fluid using the thermal energy from the turbine outlet. The evaporator produces the evaporation of the organic fluid up to the ORC turbine inlet conditions 2 and 3, by recovering the heat from the topping cycle (F-G). Thus, the vapor flows in the turbine (3–4) connected to a high-speed electric generator. At the exit of the turbine, the organic fluid goes to the hot side of the recuperator (4–5) where it is cooled to a temperature a little higher than the condensation temperature. Finally, the condenser closes the cycle (5–6).

Several methodologies have been proposed in literature to select the optimal working fluid, including mixtures and statistically advanced fluid theory [60,61] or thermo-economic optimization and cost component approaches [62]. In this case, since the temperature of the heat available from the topping cycle is relatively high, siloxanes and toluene can be considered as suitable candidates as organic fluids for the ORC cycle thanks to their high critical temperatures. Toluene has been preferred here to siloxanes as the ORC working fluid because, as described in [14,63] it was proven to give the better efficiency in energy recovery applications from hot gases exiting at 390 °C, due to its improved heat recovery coefficient. The evaporation pressure has been limited to 10 bar in order to avoid excessive volumetric ratio that affects negatively the turbine efficiency.

3.2. CSP sizing and energy yield assessment

The solar collectors are based on the ENEA technology [58] consisting of PTCs making use of sodium-/potassium-nitrate molten salts as the HTF as well as the TES medium. These salts are liquid at 240 °C and stable up to 600 °C [64]. PTC technology is the most widespread CSP solution [65,66], and the ENEA configuration adopts a receiver with a novel high efficiency selective coating that is stable up to 600 °C [67,68]. This technology is proved to be well suited to produce steam up to 550 °C.

The mirrors (1-mm thin coated glass supported by a sheet-moulding compound support panel) have a reflectivity of 95%. The TES section is a typical two-tank direct storage system, where the high temperature difference between the two tanks containing

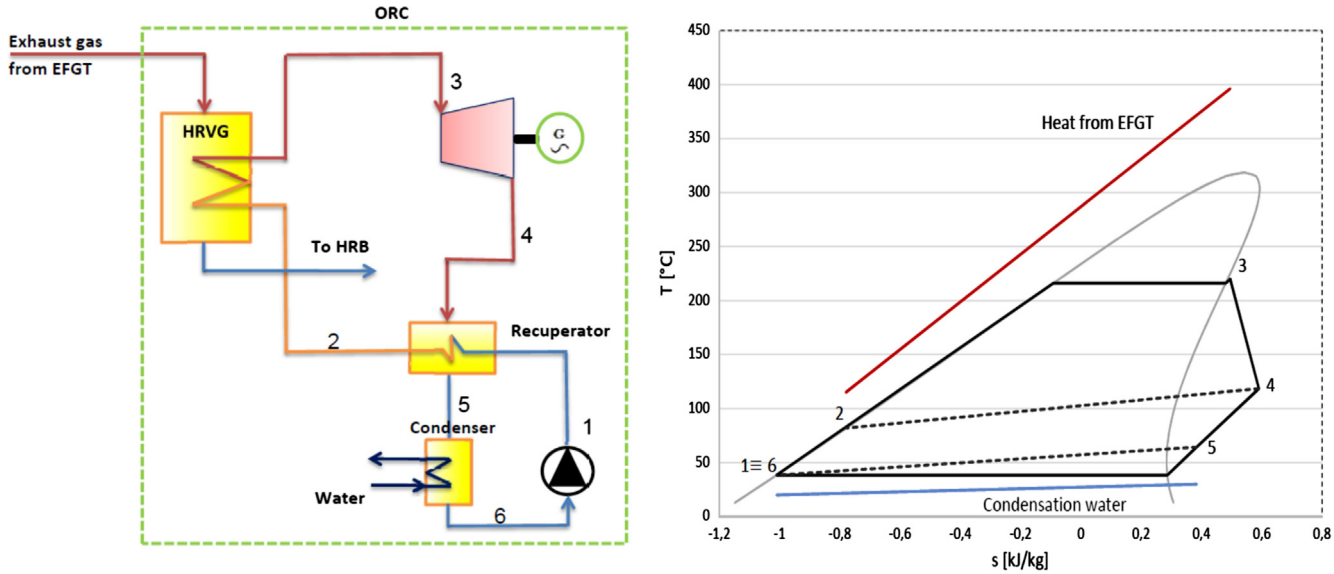

Fig. 2. Layout and *T-s* diagram ORC plant.

the molten salts (260 °C instead of 100 °C of conventional systems) allows reduced tank size and limited heat losses [68]. This technology was firstly tested at lab scale in a PTC facility at the ENEA Casaccia Research Center (Rome, Italy) and then demonstrated in the Archimede demonstration plant in Priolo Gargallo (Syracuse, Sicily, Italy) [58,59].

The solar collector field is sized to supply 50% of the total rated thermal input to the hybrid solar-biomass plant. It is assumed that the compressed air is heated in the PTC field up to 500 °C, which corresponds to a thermal energy input of 3670 kWt. The required area of the solar field is evaluated assuming a standard direct normal irradiance (DNI) of 800 W/m^2. Each solar collector has useful intercepting area of 67.3 m^2. The Solar Collector Assembly (SCA) comprises eight collectors controlled by a central driving unit, and each solar field line has eight SCAs. The net photo-thermal efficiency is 65%.

3.2.1. CSP section sizing

The solar plant is sized assuming two scenarios of 1.3 and 5.0 h of TES capacity (6-h charging time). In the first case, TES operate only as energy buffer to reduce the variability of the source and recover the energy produced by the solar field and not used. Instead, in the second scenario, TES is used to increase the solar energy utilization factor. The technical specifications of the solar field with the two different TES sizes are reported in Table 2, where the solar multiple represents the ratio between the solar collector intercepting area with and without TES. The required ground area is estimated assuming a distance between each collector line of 2.5 times the PTC aperture size.

Table 2
Characteristics of the solar field and of the thermal energy storage.

Case study	Cases B and D	Cases C and E
Design TES capacity [h]	1.3	5.0
Number of lines – total SCAs [–]	2–16	3–24
Intercepting area [m^2]	8609	12,914
Required ground area [m^2]	21,523	32,300
Intercepted solar power [MWt]	6.89	10.33
Available thermal power [MWt]	4.48	6.72
Solar multiple [–]	1.22	1.83
Thermal power to the TES [MWt]	0.81	3.04
TES capacity [MWh]	4.8	18.3

3.2.2. Solar energy yield assessment

Many models are available for the estimation of the solar radiation at different locations and the resulting CSP energy yield [69]. In this paper, the Hottel model [70] is adopted to calculate the average monthly reduction coefficient A of the monthly direct normal irradiance MDNI (kWh/m^2 month) [71].

The Aperture Normal Irradiance (ANI, in W/m^2), that is the effective irradiance normal to collectors' aperture plane, is a function of the incidence angle θ_i on the collectors' plane, the incidence angle modifier IAM, the row shadow losses and the losses from the ends of the collectors, according to Eq. (1) [72–74]:

$$\mathrm{ANI} = \mathrm{DNI} * \cos\theta_i * \mathrm{IAM} * (1 - f_{\mathrm{EndLosses}} - f_{\mathrm{RowShadow}}). \quad (1)$$

The DNI and the average Monthly Direct Normal Irradiance (MDNI, in kWh/m^2 month) is taken from [71], selecting the site of Priolo Gargallo (Siracusa, Italy, Latitude: 37°08′04″, Longitude: 15°03′00″, 30 m a.s.l., solar collector positioning N-S). Fig. 3 shows the hourly plot of DNI (with an average value of 257 W/m^2) and of ANI (average value of 201 W/m^2). The annual DNI for the site is equal to 2256 kWh/m^2 year, and the annual ANI is equal to 1760 kWh/m^2 year with a loss of 22%, as reported in Table 3.

From the known hourly ANI distribution and the total reflecting surface, it is possible to evaluate the collector efficiency distribution, the thermal energy collected and absorbed by the heat transfer fluid. The energy that can be stored in the storage system is the collected energy minus the network thermal losses. Not all the collected energy can be stored in the hot tank because of the storage capacity; part of this energy is dumped when the tank is full. With this procedure, it is possible to evaluate the energy transferred as heat input to the thermodynamic cycle and the annual energy balance of the solar plant.

Adopting the methodology proposed in [26] and assuming an annual system availability of 95%, collector thermal losses of 50 kW per line, network losses of 60 W/m (300 m pipe length), the useful solar thermal energy input to the plant results 8229 and 12,202 MWh/yr for the two assumed CSP and TES sizes (Case Studies B/D and C/E, respectively), as reported in Table 3. The rejected energy results of 6.15% and 9.44% of total collected energy on annual basis respectively for Cases B/D and C/E, while network losses and solar field

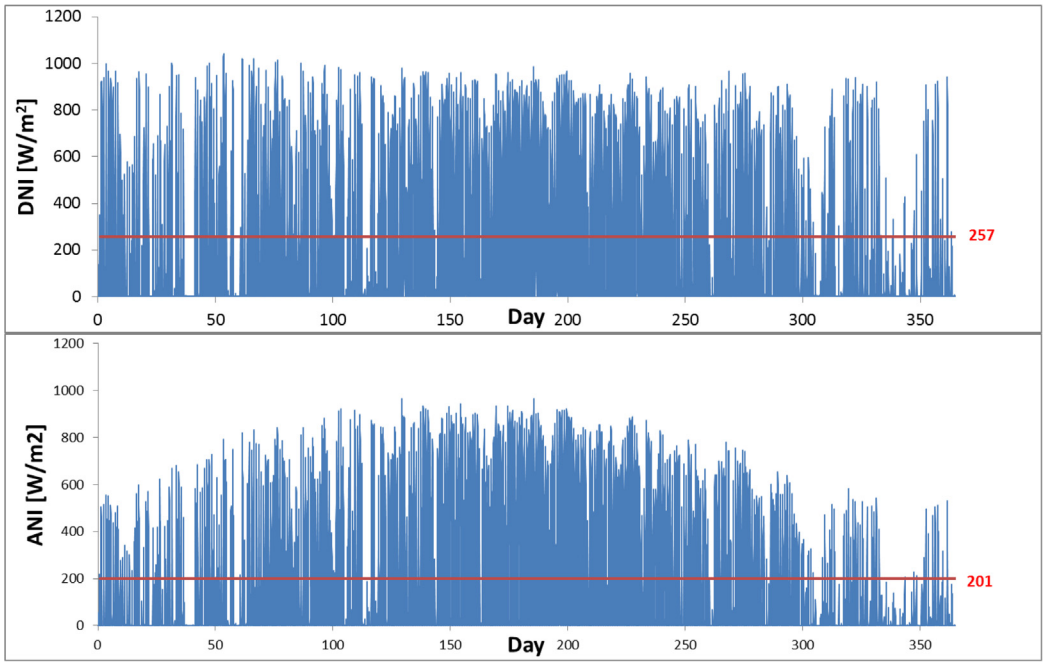

Fig. 3. Hourly DNI and ANI at the selected site of Priolo Gargallo [70].

Table 3
Monthly DNI, average monthly reduction coefficient *A*, monthly ANI and thermal energy output from the solar section.

Month	DNI [kWh/m^2]	*A* [–]	ANI [kWh/m^2]	Available energy (Cases B and D) [MWh]	Available energy (Cases C and E) [MWh]
January	124	0.48	60	279	414
February	145	0.61	88	413	613
March	183	0.76	139	650	964
April	206	0.86	178	830	1.230
May	247	0.92	227	1.063	1.576
June	253	0.92	233	1.088	1.613
July	264	0.92	243	1.136	1.684
August	235	0.90	211	989	1.466
September	190	0.80	152	711	1.055
October	168	0.67	112	525	779
November	123	0.52	64	300	444
December	117	0.45	53	246	365
Total	2256		1760	8229	12,202

losses are around 0.27% and 4.0% of the total collected energy in both cases.

Table 4 reports the rated performance results from the thermodynamic simulation with and without CSP.

Table 4
Rated performance of the proposed case studies as resulting from the simulation.

Parameter	Unit	EFGT + ORC Biomass-Only	Hybrid CSP + Biomass
EFGT electric power output	kWe	1388	1388
ORC cycle power output	kWe	700	700
Total electric power output (ISO)	kWe	2083	2083
Auxiliary consumption (in % of rated power)	%	6	10
Available thermal power output (CHP)	kWt	963	963
Biomass consumption	kg/s	1	0.5
Biomass thermal power (referred to LHV)	kWt	9050	4523
Thermal power produced by CSP plant	kWt	–	3673
Overall electric efficiency (referred to biom. LHV)	%	23.0	46.0

3.3. Thermodynamic analysis results

The modelling results report a net electric efficiency (defined as the total generated electricity as a fraction of the input biomass energy at nominal solar-energy input, delivered to the grid, not considering auxiliary consumption) of 23% for the 100% biomass plant of Case A (no solar contribution), and of 46% for the hybrid cycles of Cases B to E. An energy breakdown of the plant at the rated operating conditions (baseload with solar input of 3673 kW) is given in Fig. 4. The thermodynamic analysis has been carried out by means of Cycle-tempo [75] and considering the total thermal input as the sum of the biomass thermal power (given by the rated power of 4523 kWt referred to the biomass LHV) and the thermal power of 3673 kWt delivered by the solar plant to the EFGT, as detailed in Table 4.

It appears that 25% of the total energy input is converted to electrical power, while 8% can be used for thermal uses from gas exiting the HRVG and a further 18% can be used from the heat rejected at the compressor intercooler. The heat rejected at the condenser, and the heat exhausted to the atmosphere from the gas exiting from the furnace and from the air exiting the HRB can-

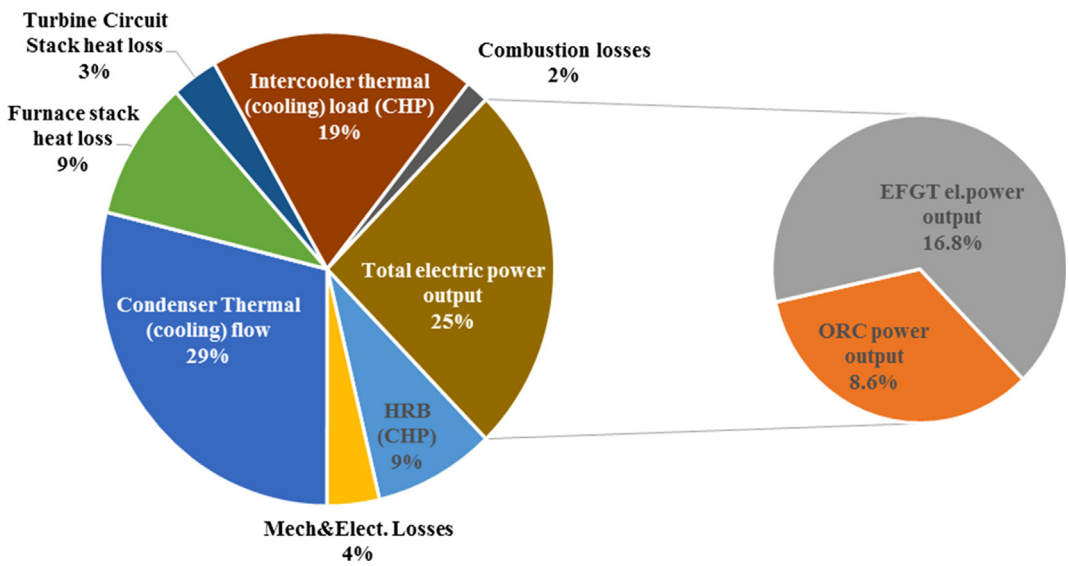

Fig. 4. Overall plant energy balance; share of rated thermal and electrical power outputs with respect to the total thermal input (sum of the Biomass thermal power, 4523 kWt, and CSP thermal power, 3673 kWt, as detailed in Table 4).

Table 5
Overview of the five case studies considered in the present work.

Case study	A	B	C	D	E
Biomass furnace rated thermal power [kW_t]	9050	9050	9050	4523	4523
Biomass input [t/yr]	25,694	22,865	21,462	13,999	13,999
Net electricity generation [MWh/yr]	15,741	15,741	15,741	10,761	11,818
Equivalent operating hours [h/yr]	8040	8040	8040	5496	6036

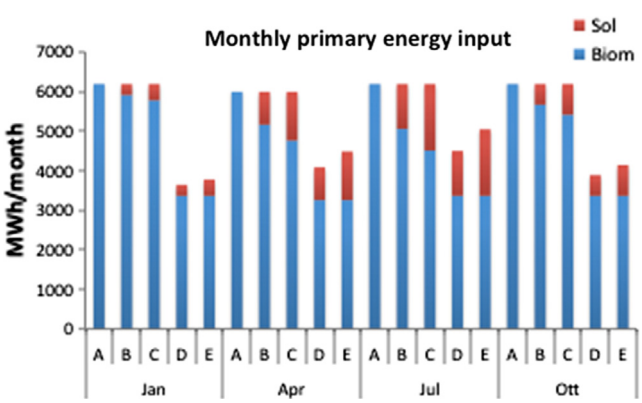

Fig. 5. Monthly primary energy contribution from biomass and solar source in four different months of the year for the proposed case studies.

not be used for cogeneration because their temperature is too low for further thermal uses. In generating these results, the part load efficiency of the biomass boiler in Cases B and D has been neglected.

Salient results relating to all five selected case studies are summarized in Table 5. The 100% biomass-only plant (Case A) as well as Case B and C, which have fixed power outputs with a modulating biomass boiler to compensate the variable solar input, have biomass boiler thermal loads of 9.05 MWt. Cases D and E, in which the plant has a variable output with a fixed biomass input (50% of nominal CHP output), have lower biomass boiler thermal loads of 4.52 MWt. The corresponding net electricity generation from the plants amounts to 15.7 MWh/yr in Cases A, B and C, which also have a little over 8000 operating hours per year, 10.8 MWh/yr in Case D (close to 5500 h/yr), and 11.8 MWh/yr in Case E (close to 6000 h/yr). The primary energy inputs from the biomass and solar sources in different months of the year are reported in Fig. 5. From Fig. 5, it can be seen that the primary solar-energy contribution is generally small in all cases.

Table 6
Main characteristics of the plant heat exchangers.

Component	Low-end ΔT [K]	High-end ΔT [K]	Heat flow [kW]	Log. ΔT_{lm} [K]	UA [kW/K]	U [W/(m^2 K)]	A [m^2]
Intercooler	15	132	1590	53.8	29.6	45	656.8
Condenser	18.96	8.96	2377.46	13.3	178.2	1000	178.2
Air pre-heater	125.67	34.56	2396.72	70.6	34.0	30	1132.0
ORC recuperator	25.0	36.5	410	30.4	13.5	60	225.0
HRVG	33	176.19	3155.77	85.5	36.9	300	123.1
HTHE (gas–gas)	30	241.31	3654.45	101.4	36.1	30	1201.9
HRB	10.0	64.9	708	29.4	24.1	100	241.1
Solar salts (HTF)-gas	110.0	50.0	3660	76.1	48.1	55	874.5

Finally, Table 6 shows the results of the calculations regarding the heat exchangers. The overall heat transfer coefficients are estimated for the different cases on the basis of the values suggested in Ref. [75]. All the surfaces are evaluated considering the operating conditions with solar input (Case B), except than the HTHE that has been designed considering the operating conditions with only biomass (Case A). It appears from these results that the gas-gas heat exchangers, as expected, need the largest heat transfer surfaces and, therefore, represent the largest costs of the plant.

4. Thermo-economic analysis

A profitability assessment of the hybrid CSP-biomass combined EFGT-ORC CHP plant is performed in this section. For each case study, the scenarios of electricity-only generation and cogeneration of heat and power, as well as a sensitivity analysis to the heat demand intensity and the biomass purchase price, are considered. A basic strategy is assumed here of electricity fed into the grid, given that CHP plants are eligible for FiTs in the Italian energy market where this study is focused.

4.1. Costs assessment

The turnkey costs were estimated by means of interviews and data collection from manufacturers of the selected technologies [14]. In particular, the following sources have been considered: Saturn 20 Solar Turbines; Turboden for the ORC genset; Uniconfort for biomass boiler, hot air genset and heat exchanger (maximum temperature of 800 °C). For the CSP section, PTCs and TES costs were derived from NREL cost figures [76–78], according to the lessons learnt from ENEA/Enel Archimede project [15]. In particular, unitary PTC costs of 250 Eur/m^2, TES costs of 25 kEur/MWh and a 30% cost increase for installation, piping and the HTF are assumed. The capex and opex cost items are summarized in Table 7. The annual O&M costs are assumed 4% of the turnkey cost and the ash discharge are accounted for assuming unitary cost of 70 Eur/t ash. Personnel costs are included at a rate of 268 kEur/yr [14].

From Table 7, the total predicted turnkey cost is lowest at 4.7 MEur for Case A, which is the biomass-only plant (Case A) that does not have a solar field, and is highest at 9.5 MEur for Case C, which features significant TES and a fixed power output with a modulating biomass boiler and a variable solar input. From the results in this table it can be seen that variable power output hybrid plants and, even more so, plants with a smaller TES capacity are generally associated with lower turnkey costs. This is also reflected in the upfront specific costs (in kEur/kWe), which vary from 2.3 kEur/kWe for the biomass-only plant (Case A) to 4.5 kEur/kWe for the hybrid plant of Case C.

Opex, on the other hand, varies from a high of 2.3 kEur/yr for the biomass-only plant (Case A) to a low of 1.5 kEur/yr for the plant of Case C, given the larger volume of biomass (fuel) required in the former. The results reveal that variable power output plants are generally associated with lower operating costs, whereas the degree of available TES in the plant (Case B *vs.* C, and Case D *vs.* E) does not have a significant effect on this cost component (to within a few% points).

4.2. Energy revenues and financial assumptions

The financial appraisal of the investment is carried out assuming the following hypotheses: (i) 20 years of operating life and FiT duration for renewable electricity; no 're-powering' throughout the 20 years; zero decommissioning costs, straight line depreciation of capital costs over 20 years; (ii) maintenance costs, fuel supply costs, electricity and heat selling prices held constant (in real 2017 values); (iii) cost of capital (net of inflation) equal to 5%, corporation tax neglected, no capital investments subsidies. Electricity is sold to the grid at the feed-in electricity price available in the Italian energy market [79], which is 180 and 296 Eur/MWh respectively for biomass electricity (assuming the use of lignocellulosic by-products in the form of wood chips from forestry harvesting) and CSP electricity. These figures are valid in the considered power size range, TES size, adoption of best available technologies for air emissions abatement, and use of agricultural by-products from

Table 7
Capex and opex costs assumptions for the hybrid combined cycle.

Case study	A	B	C	D	E
Turnkey cost (kEur):	4700	7684	9450	7284	9050
– PTC field and CSP installation	–	2863	4294	2863	4294
– TES	–	121	456	121	456
– Gas turbine	1200	1200	1200	1200	1200
– ORC genset	1200	1200	1200	1200	1200
– Biomass furnace	1000	1000	1000	600	600
– HTHE for EFGT	600	600	600	600	600
– Civil work, grid connection, engine, development	700	700	700	700	700
Upfront cost [kEur/kWe]	2.26	3.69	4.54	3.50	4.34
Opex (incl. fuel) [kEur/yr]	2285	2186	2099	1532	1549

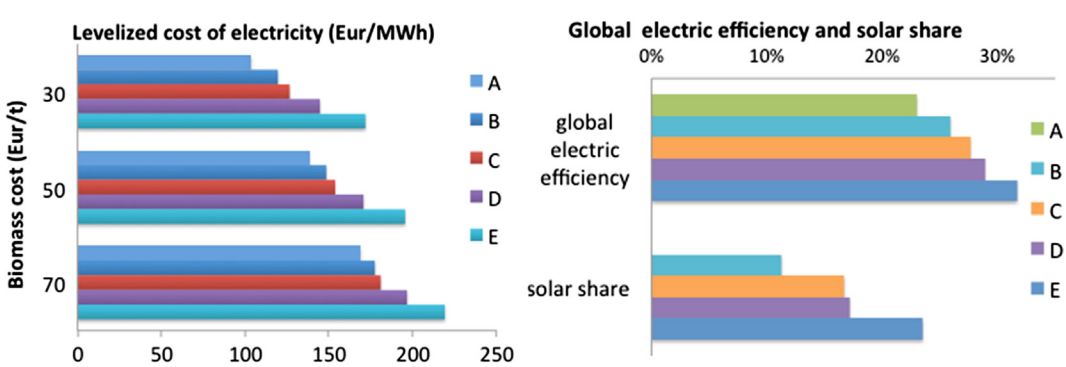

Fig. 6. LCOE as a function of the biomass purchase price (left) and energy balances as resulting from the thermodynamic modelling (right) of Cases A to E.

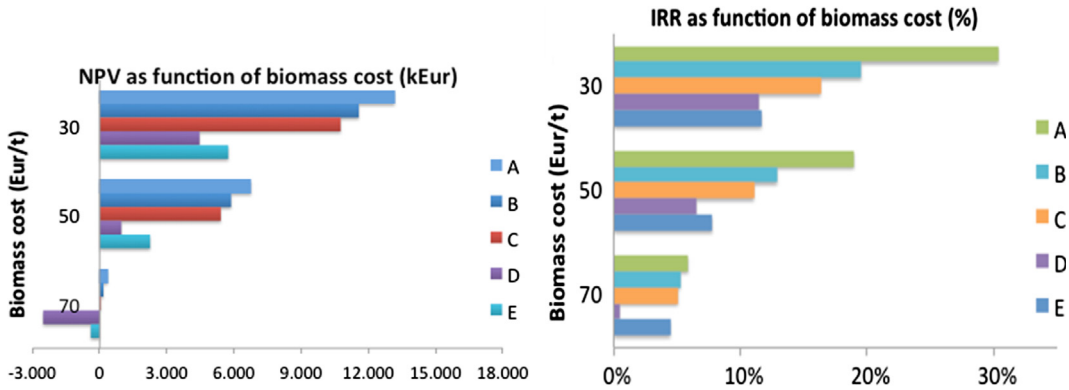

Fig. 7. NPV (left) and IRR (right) for Cases A to E as a function of biomass supply cost for electricity-only generation scenario.

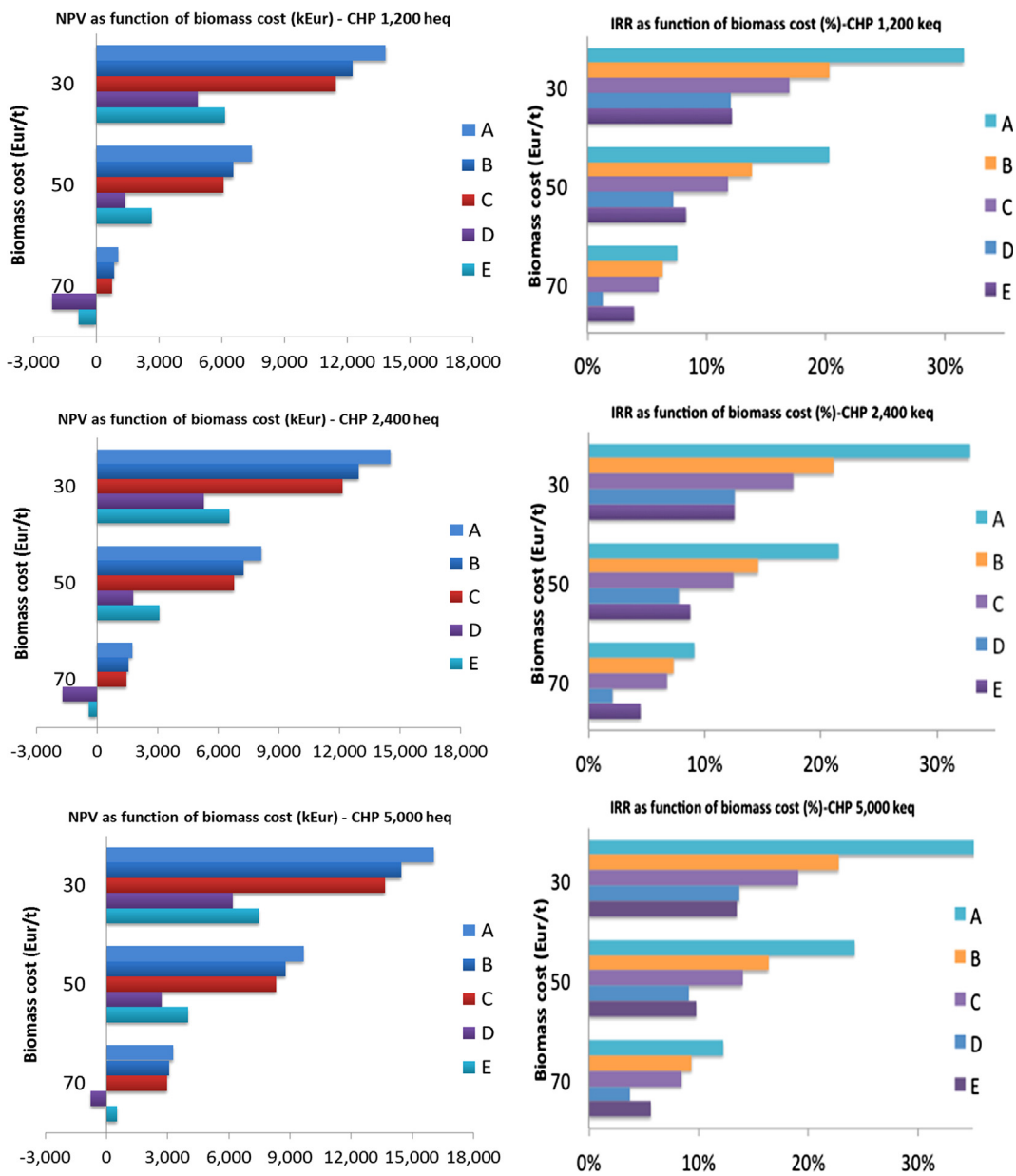

Fig. 8. NPV (left) and IRR (right) as a function of heat demand (equivalent h/yr) and biomass supply cost in CHP scenario.

local and sustainable supply chains [79]. The electricity generation is calculated at 8040 operating hours per year. Cogenerated thermal energy is sold at a price of 80 Eur/MWh.

5. Energy performance and profitability assessment results

Fig. 6 shows the energy performance, specifically in terms of the global electricity efficiency and solar share, and LCOE at different biomass supply costs, in the case of electricity-only/power-genera tion production. The global electricity efficiency is the ratio of electricity annual sales and biomass energy input, while the solar share is the percentage of solar energy input on a yearly basis. Furthermore, the profitability assessment results are shown in Figs. 7 and 8, which report respectively the Net Present Value (NPV) and Internal Rate of Return (IRR) as a function of the biomass supply cost, for both electricity-only and cogeneration scenarios (in this case varying the equivalent heat-demand hours, which represent the ratio of annual thermal energy delivered to the load and thermal power of CHP plant).

Of interest is to observe the emerging LCOE values, which are from around 100 Eur/MWh to above 220 Eur/MWh. Moreover, NPV values from close to 13,000 kEur to −3000 kEur and IRR values from 30% down to almost zero when prioritizing electrical power generation (i.e., not in cogenerative mode). The hybridization of the biomass EFGT with CSP increases the global electricity efficiency, due to the reduced biomass requirement, but reduces the NPV and IRR in all scenarios. In fact, despite the increased global energy efficiency of the solar input, and the higher electricity selling price of the solar based fraction on respect to biomass based one, the investment costs of the PTCs with molten salts as HTF are very high and make this investment not competitive. This is more evident at higher solar shares (Cases C and E, in comparison to Cases B and D) where the larger PTC solar-array areas (and consequently higher investment costs) make the investment less profitable. Moreover, the option of fixed biomass furnace-load operation and variable electricity output (on the basis of the variable solar-energy input) of Cases D and E is also less profitable than the corresponding cases of baseload operation (Cases B and C), despite being more efficient for the higher solar share. Only in the case of variable energy output with fixed biomass input (Cases D and E), the investment profitability increases with the solar section size (from Cases D to E) and this is due to the higher revenues from electricity sales that compensate the relatively higher investment cost for the solar PTC. This is more evident at higher biomass supply costs.

In general, the results indicate the reduced economic viability of CSP integration into biomass-only plants, due to high investment costs of the former which are not compensated by the higher global energy conversion efficiency and additional sales revenues, but alternatively, the same finding implies an improved economic viability of integrating biomass-firing in combined thermal-CSP plants.

6. Conclusions

A thermodynamic and economic analysis has been performed on a hybrid (solar-biomass) combined cycle featuring by a PTC field with molten salts as the HTF delivered at a maximum temperature of 550 °C, upstream of a 4.5–9 MWt fluidized-bed biomass combustor, with thermal energy storage. the heat sources drive an EFGT top cycle and a bottoming ORC unit with a total of 2.1 MWe and 960 kWt generated, of which 1.4 from EFGT and 0.7 from the bottoming ORC. The thermodynamic modelling has been performed assuming two different CSP sizes, storage levels and a fixed or modulating biomass combustor operation mode. in particular, the CSP collector array covers a total ground area of 22,000–32,000 m^2, and the two molten-salt tanks considered can provide 4.8–18 MWh (corresponding to 1.3–5.0 h) of thermal energy storage as a means of reducing the variations in the plant's operating conditions, increasing the plant's capacity factor and total equivalent operating hours (from 5500–6000 to 8000 h per year). On the basis of the results of the thermodynamic simulations, upfront and operational costs assessments, and considering an Italian energy policy scenario (feed-in tariffs, or FiTs, for renewable electricity), the global energy conversion efficiency and investment profitability of this plant are estimated for different sizes of CSP and biomass furnaces, different operation strategies (baseload and modulating) and cogenerative *vs*. electricity-only system configurations. upfront costs in the range 4.3–9.5 MEur are reported, with operating costs in the range 1.5–2.3 MEur annually. Levelized costs of energy from around 100 eur/MWh to above 220 Eur/MWh are found, along with net present values (NPVs) from close to 13,000 to −3000 kEur and internal rates of return (IRRs) from 30% down to almost zero when prioritizing electrical power generation (i.e., not in cogenerative mode). The energy performance results present higher global conversion efficiencies when using CSP integration but the thermo-economic analysis reports a lower NPV and IRR of the investment when integrating solar energy, in the selected rage of biomass supply cost (30–70 Eur/t), and this is due to the higher investment costs of solar *vs*. biomass sections that are not compensated by the relatively higher selling price of solar-based *vs*. biomass-based electricity. A baseload operation strategy, which maximizes the electricity output and compensates the solar energy fluctuations with a modulating biomass furnace, proves to be the most profitable hybridization option (despite being less efficient in terms of global energy performance) in comparison to a strategy with a fixed biomass consumption rate and variable electricity output on the basis of solar radiation levels in all cases the economic viability of the systems deteriorate for larger CSP section sizes. The results indicate the low economic profitability of CSP integration in comparison to biomass-only plants, due to high investment costs of the former, which are not compensated by the higher global energy conversion efficiency and energy sales revenues. However, these results could be significantly different if a flexible operation of dispatchable hybrid solar-biomass CHP will be properly rewarded in a future energy framework and a proper integration of renewable on site CHP operational strategies and demand response solutions will be incentivized, in light of increased flexibility of energy systems and enhanced integration of intermittent and programmable energy sources, active network management and demand side management options. Future researches regard different CSP-biomass hybridization configurations, in order to increase energy conversion efficiency and flexibility, such as solar energy input feeding directly a bottoming ORC instead of integrating the biomass energy stream to the topping EFGT.

Acknowledgments

This work was also supported by the UK Engineering and Physical Sciences Research Council (EPSRC) [Bioenergy value chains: while system analysis and optimization, grant number EP/K036734/1]. Data supporting this publication can be obtained on request from cep-lab@imperial.ac.uk.

References

[1] European Commission. <http://ec.europa.eu/clima/news/articles/news_2014102401_en.htm>; 2014 [accessed April 2017].
[2] Markides CN. Low-concentration solar-power systems based on organic Rankine cycles for distributed-scale applications: Overview and further developments. Front Energy Res 2016;3(47):1–16. http://dx.doi.org/10.3389/fenrg.2015.00047.

[3] Liu M, Steven Tay NH, Bell S, Belusko M, Jacob R, Will G, et al. Review on concentrating solar power plants and new developments in high temperature thermal energy storage technologies. Renew Sustain Energy Rev 2016;53:1411–32.
[4] Peterseim JH, White S, Tadros A, Hellwig U. Concentrated solar power hybrid plants, which technologies are best suited for hybridisation? Renewable Energy 2013;57:520–32.
[5] Pantaleo AM, Giarola S, Bauen A, Shah N. Integration of biomass into urban energy systems for heat and power. Part I: An MILP based spatial optimization methodology. Energy Convers Manage 2014;83:347–61. http://dx.doi.org/10.1016/j.enconman.2014.03.050.
[6] Pantaleo AM, Giarola S, Bauen A, Shah N. Integration of biomass into urban energy systems for heat and power. Part II: Sensitivity assessment of main techno-economic factors. Energy Convers Manage 2014;83:362–76. http://dx.doi.org/10.1016/j.enconman.2014.03.051.
[7] Amirante R, Clodoveo ML, Distaso E, Ruggiero F, Tamburrano P. A tri-generation plant fuelled with olive tree pruning residues in apulia: An energetic and economic analysis. Renewable Energy 2016;89:411–21. http://dx.doi.org/10.1016/j.renene.2015.11.085.
[8] Amirante R, Tamburrano P. Novel, cost-effective configurations of combined power plants for small-scale cogeneration from biomass: Feasibility study and performance optimization. Energy Convers Manage 2015;97:111–20. http://dx.doi.org/10.1016/j.enconman.2015.03.047.
[9] Amirante R, Cassone E, Distaso E, Tamburrano P. Overview on recent developments in energy storage: Mechanical, electrochemical and hydrogen technologies. Energy Convers Manage 2017;132:372–87. http://dx.doi.org/10.1016/j.enconman.2016.11.046.
[10] Anuradha Mishra M, Chakravarty N, Kaushika N. Thermal optimization of solar biomass hybrid cogeneration plants. J Sci Ind Res 2006;65(4):355–63.
[11] Freeman J, Hellgardt K, Markides CN. An assessment of solar-powered organic Rankine cycle systems for combined heating and power in UK domestic applications. Appl Energy 2015;138:605–20. http://dx.doi.org/10.1016/j.apenergy.2014.10.035.
[12] Freeman J, Hellgardt K, Markides CN. Working fluid selection and electrical performance optimisation of a domestic solar-ORC combined heat and power system for year-round operation in the UK. Appl Energy 2017;186:291–303. http://dx.doi.org/10.1016/j.apenergy.2016.04.041.
[13] Freeman J, Hellgardt K, Markides CN. An assessment of solar–thermal collector designs for small-scale combined heating and power applications in the United Kingdom. Heat Transf Eng 2015;36(14–15):1332–47. http://dx.doi.org/10.1080/01457632.2015.995037.
[14] Camporeale S, Pantaleo A, Ciliberti P, Fortunato B. Cycle configuration analysis and techno-economic sensitivity of biomass externally fired gas turbine with bottoming ORC. Energy Convers Manage 2015;105:1239–50.
[15] Miliozzi A, Liberatore R, Giannuzzi GM, Veca E, Nicolini D, Lanchi M, et al. ENEA research and innovation on Thermal Energy Storage for CSP plants. In: 16th CIRIAF National Congress, Assisi (PG, Italy), 7–9 April..
[16] Srinivas T, Reddy BV. Hybrid solar-biomass power plant without energy storage. Case Stud Therm Eng 2014;2:75–81.
[17] Servert J, San Miguel G, López D. Hybrid Solar - Biomass Plants for Power Generation. Tech Econ Assess, Global NEST J 2011;13(3):266–76.
[18] Al-attab KA, Zainal ZA. Externally fired gas turbine technology: A review. Appl Energy 2015;138:474–87. http://dx.doi.org/10.1016/j.apenergy.2014.10.049.
[19] Pantaleo A, Pellerano A, Carone MT. Potentials and feasibility assessment of small scale CHP plants fired by energy crops in Puglia region (Italy). Biosys Eng 2009;102(3):345–59. http://dx.doi.org/10.1016/j.biosystemseng.2008.12.002.
[20] Barigozzi GG, Bonetti GG, Franchini GG, Perdichizzi AA, Ravelli SS. Solar hybrid combined cycle performance prediction: influence of GT model and spool arrangement. ASME. Turbo Expo: Power for Land, Sea, and Air, Volume 6: Oil and Gas Applications; Concentrating Solar Power Plants; Steam Turbines; Wind Energy; 2012. p. 291–301. doi: http://dx.doi.org/10.1115/GT2012-68881.
[21] IRENA. Concentrating solar power, renewable energy technologies: cost analysis series, Volume 1: Power Sector, Issue 2/5, June 2012; 2012.
[22] Barua A, Chakraborti S, Paul D, Das P. Analysis of concentrated solar power technologies feasibility, selection and promotional strategy for Bangladesh. J. Mech. Eng. 2014;ME 44(2).
[23] Jamel M, Rahman AA, Shamsuddin AH. Advances in the integration of solar thermal energy with conventional and non-conventional power plants. Renew Sustain Energy Rev 2013;20:71–81. http://dx.doi.org/10.1016/j.rser.2012.10.027.
[24] Santos MJ, Merchán RP, Medina A, Calvo Hernández A. Seasonal thermodynamic prediction of the performance of a hybrid solar gas-turbine power plant. Energy Convers Manage 2016;115:89–102.
[25] Vidal M, Martin M. Optimal coupling of a biomass based polygeneration system with a concentrated solar power facility for the constant production of electricity over a year. Comput Chem Eng 2015;72:273–83.
[26] Peterseim JH, White S, Tadros A, Hellwig U. Concentrating solar power hybrid plants - Enabling cost effective synergies. Renewable Energy 2014;67:178–85. http://dx.doi.org/10.1016/j.renene.2013.11.037.
[27] Pérez Á, Torres N. Solar parabolic trough and biomass hybrid plants: a cost efficient concept suitable for places in low irradiation conditions. In: Solar-PACES Conf, 21-23 Sept, Perpignan. p. 21–3.
[28] Peterseim JH, Tadros A, White S, Hellwig U, Klostermann F. Concentrated solar power/energy from waste hybrid plants e creating synergies. In: SolarPACES conference.
[29] Okoroigwe E, Madhlopa A. An integrated combined cycle system driven by a solar tower: a review. Renew Sust Energy Rev 2016;57:337–50.
[30] Spelling J. Hybrid solar gas-turbine power plants Ph.D. thesis. Stockholm, Sweden: KTH Royal Institute of Technology, Department of Energy Technology; 2013.
[31] Barigozzi G, Perdichizzi A, Gritti C, Guaiatelli I. Techno-economic analysis of gas turbine inlet air cooling for combined cycle power plant for different climatic conditions. Appl Therm Eng 2015;82:57–67.
[32] Okoroigwe E, Madhlopa A. Evaluation of the potential for hybridization of gas turbine power plants with renewable energy in South Africa. IEEE conference publications 2015. http://dx.doi.org/10.1109/DUE.2015.7102985.
[33] Li Y, Liao S, Liu G. Thermo-economic multi-objective optimization for a solar-dish Brayton system using NSGA-II and decision making. Elect Power Energy Syst 2015;64:167–75.
[34] Schwarzbözl P, Buck R, Sugarmen C, Ring A, Marcos Crespo M, Altwegg P, et al. Solar gas turbine systems: design, cost and perspectives. Sol Energy 2006;80:1231–40 [4].
[35] Barigozzi G, Bonetti G, Franchini G, Perdichizzi A, Ravelli S. Thermal performance prediction of a solar hybrid gas turbine. Sol Energy 2012;86:2116–27.
[36] Soares J, Oliveira AC. Numerical simulation of a hybrid concentrated solar power/biomass mini power plant. Appl Therm Eng 2016;111:1–10. http://dx.doi.org/10.1016/j.applthermaleng.2016.06.180.
[37] Collado F, Guallar J. A review of optimized design layouts for solar power tower plants with campo code. Ren Sust Energy Rev 2013;20:142–54.
[38] Solar Borges. <https://www.nrel.gov/csp/solarpaces/project_detail.cfm/projectID=242>.
[39] Nixon J, Dey P, Davies P. The feasibility of hybrid solar-biomass power plants in India. Energy 2012;46(1):541–54.
[40] Shaheen Hasan C, Amanullah MT, Palash KB. Biomass supported solar thermal hybrid power plant for continuous electricity generation from renewable sources. In: ICDRET 2012: Proceedings of the Developments in Renewable Energy Technology 2012 International Conference. Piscataway, N.J.: IEEE; 2012. p. 57–60.
[41] Schnatbaum L. Biomass utilization for Co firing in parabolic trough power plants. In: SolarPACES conference.
[42] Piemonte V, Falco MDe, Tarquini P, Giaconia A. Life Cycle Assessment of a high temperature molten salt concentrated solar power plant. Sol Energy 2011;85(5):1101–8. http://dx.doi.org/10.1016/j.solener.2011.03.002.
[43] Amoresano A, Langella G, Sabino S. Optimization of solar integration in biomass fuelled steam plants. Energy Procedia 2015;81:390–8.
[44] Wang X, Liu Q, Bai Z, Lei J, Jin H. Thermodynamic Analysis of the Cascaded Supercritical CO2 Cycle Integrated with Solar and Biomass Energy. In: ICAE 2016 Conference, Bejing 8–11 october.
[45] Merchán RP, Santos MJ, Medina A, Hernández AC. Thermodynamic Model of a Hybrid Brayton Thermosolar Plant. In: Proceedings of ECOS 2016, Portoroz, SL, 19–23 june.
[46] Burin EK, Buranello L, Giudice P Lo, Vogel T, Grner K, Bazzo E. Boosting power output of a sugarcane bagasse cogeneration plant using parabolic trough collectors in a feedwater heating scheme. Appl Energy 2015;154:232–41. http://dx.doi.org/10.1016/j.apenergy.2015.04.100.
[47] Yue T, Lior N. Thermodynamic analysis of solar-assisted hybrid power generation systems integrated with thermochemical fuel conversion. Energy 2016;191:204–22. http://dx.doi.org/10.1016/j.energy.2016.10.093.
[48] Bai Z, Liu Q, Lei J, Hong H, Jin H. New solar-biomass power generation system integrated a two-stage gasifier. Appl Energy 2016;194:310–9. http://dx.doi.org/10.1016/j.apenergy.2016.06.081.
[49] Barlev D, Vidu R, Pieter Stroeve I. Innovation in concentrated solar power. Solar Energy Mater Sol Cells 2011;95:2703–25.
[50] European Concentrated Solar Thermal Road-Mapping, SES6-CT-2003-502578, DLR <http://www.promes.cnrs.fr/uploads/pdfs/ecostar/ECOSTAR.Roadmap.pdf>; 2005.
[51] ProtermoSolar. Mapa de la Industria Solar Termoelectrica en Espana. <http://www.protermosolar.com/mapa.html>; 2012.
[52] Patnode AM. Simulation and Performance Evaluation of Parabolic Trough Solar Power Plant, NREL-2006.
[53] Rovira A, Barbero R, Montes MJ, Abbas R, Varela F. Analysis and comparison of Integrated Solar Combined Cycles using parabolic troughs and linear Fresnel reflectors as concentrating systems. Appl Energy 2016;162:990–1000.
[54] NREL Concentrating solar power projects URL. <http://www.nrel.gov/csp/solarpaces/> [accessed April 2017].
[55] Soltani R, Keleshtery P, Vahdati M, Khoshgoftar Manesh M, Rosen M, Amidpour M. Multi-objective optimization of a solar-hybrid cogeneration cycle: application to CGAM problem. Energy Convers Manage 2014;81:60–71.
[56] Kearney D, Kroizer I, Miller C, Steele D. Design and Preliminary Performance of Solar Electric Generation Station I at Daggett-California. In: Proc. 9th ISES congress, Canada. p. 1424–8.
[57] Pacheco JE. Final test and evaluation results from the Solar II project, SAND2002-0120; 2002.
[58] ENEA Report Solar thermal energy production: guidelines and future programmes of ENEA. <http://www.solaritaly.enea.it/Documentazione/Documentazione.php>; 2001.
[59] Archimede Solar power plant. <http://www.archimedesolarenergy.it/en_home.asp> [acc April 2017].

[60] Oyewunmi OA, Taleb AI, Haslam AJ, Markides CN. An assessment of working-fluid mixtures using SAFT-VR Mie for use in organic Rankine cycle systems for waste-heat recovery. Comput Therm Sci 2014;6(4):301–16.
[61] Oyewunmi OA, Taleb AI, Haslam AJ, Markides CN. On the use of SAFT-VR Mie for assessing large-glide fluorocarbon working-fluid mixtures in organic Rankine cycles. Appl Energy 2016;163:263–82. http://dx.doi.org/10.1016/j.apenergy.2015.10.040.
[62] Oyewunmi OA, Markides CN. Thermo-Economic and Heat Transfer Optimization of Working-Fluid Mixtures in a Low-Temperature Organic Rankine Cycle System. Energies 2016;9(6). 448:1–21.
[63] Pantaleo AM, Camporeale SM, Shah N. Thermo-economic assessment of externally fired micro-gas turbine fired by natural gas and biomass : Applications in Italy. Energy Conversion and Management 2013;75:202–13.
[64] Turchi C, Mehos M, Ho CM, Holb GJ. Current and future costs for parabolic trough and power tower systems in the US market. In: SolarPaces 2010, Perpignan, FR, September 21–24.
[65] Technology Roadmap. Concentrating Solar Power, International Energy Agency; 2010.
[66] Giannuzzi GM, Majorana CE, Miliozzi A, Salomoni VAL, Nicolini D. Structural design criteria for steel components of parabolic-trough solar concentrators. Journal of Solar Energy Engineering 2007;129:382–90.
[67] Salomoni VA, Majorana CE, Giannuzzi GM, Miliozzi A, Nicolini D. New Trends in Designing Parabolic trough Solar Concentrators and Heat Storage Concrete Systems in Solar Power Plants. In: Rugescu Radu D, editor. Solar Energy. InTech; 2010. ISBN: 978-953-307-052-0.
[68] Herrmann U, Kelly B, Price H. Two-tank molten salt storage for parabolic trough solar power plants. Energy 2004;29(5–6):883–93.
[69] Duffie JA, Beckman WA. Solar Engineering of Thermal Processes. 2nd ed. NEW YORK, NY, US: John Wiley & SONS INC.; 1991.
[70] Hottel, Woertz. Thermal theory and modeling of solar collectors. Cambridge MA: MIT press; 1990.
[71] www.solaritaly.enea.it [accessed April 2017].
[72] Patnode A. Simulation and Performance Evaluation of Parabolic Trough Solar Power Plants, Ph.D. Thesis. University of Wisconsin-Madison; 2006.
[73] Wagner MJ, Gilman P. Technical Manual for the SAM. Physical Trough Model, Technical Report, NREL/TP-5500-51825; 2011.
[74] Stine WB, Geyer M. Power From The Sun, online book, <www.powerfromthesun.net>.
[75] http://www.asimptote.nl/software/cycle-tempo.
[76] Turchi C, Mehos M, Ho CK, Kolb GJ. Current and future costs for parabolic trough and power tower systems in the US market, NREL/CP-5500-49303, SolarPACES 2010, Perpignan, France, September 21–24, 2010.
[77] Turchi C. Parabolic Trough Reference Plant for Cost Modeling with the Solar Advisor Model (SAM). Technical Report, NREL/TP-550-47605; July 2010.
[78] Sargent and Lundy Consulting Group. "Assessment of Parabolic Trough and Power Tower Solar Technology Cost and Performance Forecasts", NREL SL-5641, Chicago, IL, USA; May 2003.
[79] Italian Ministry of Economic Development, Incentives for energy from electric not-photovoltaic renewable sources, Legislative decrees of 23.06.2016.